JSES International 8 (2024) 1248–1258

Contents lists available at ScienceDirect

JSES International

journal homepage: www.jsesinternational.org

Virtual assessment of internal rotation in reverse shoulder arthroplasty based on statistical shape models of scapular size

Lisa A. Galasso, MD[a], Alexandre Lädermann, MD[b,c,d], Brian C. Werner, MD[e], Stefan Greiner, MD[f,g], Nick Metcalfe, BS[h], Patrick J. Denard, MD[a,*], Shoulder Arthroplasty Research Committee (ShARC)[b]

[a]*Oregon Shoulder Institute, Medford, OR, USA*
[b]*Division of Orthopaedics and Trauma Surgery, Hôpital de La Tour, Meyrin, Switzerland*
[c]*Division of Orthopaedics and Trauma Surgery, Department of Surgery, Geneva University Hospitals, Geneva, Switzerland*
[d]*Faculty of Medicine, University of Geneva, Geneva, Switzerland*
[e]*Department of Orthopedics, University of Virginia, Charlottesville, VA, USA*
[f]*Sporthopaedicum, Straubing and Regensburg, Germany*
[g]*Department of Trauma Surgery, University Medical Center Regensburg, Regensburg, Germany*
[h]*Arthrex, Inc., Naples, FL, USA*

ARTICLE INFO

Keywords:
Shoulder arthroplasty
Virtual
Preoperative planning
Internal rotation
Range of motion
Lateralization
Offset
Scapula size

Level of evidence: Basic Science Study; Computer Modeling

Background: The purpose of this study was to assess impingement-free internal rotation (IR) in a virtual reverse shoulder arthroplasty simulation using a Statistical Shape Model based on scapula size.
Methods: A database of over 10,000 scapulae utilized for preoperative planning for shoulder arthroplasty was analyzed with a Statistical Shape Model to obtain 5 scapula sizes including the mean and 2 standard deviations. For each scapula model, one glenosphere size (33-42 mm) was selected as the best fit based on consensus among 3 shoulder surgeons. Virtual implantation variables included 1) lateral offset (0-12 mm in 2-mm increments), 2) inferior eccentricity (0, 2.5, 5, and 7.5 mm), and 3) posterior eccentricity (0, 2.5, and 5 mm). The neck shaft angle was fixed at 135° with an inlay design humeral prosthesis. IR at the side (IR0) and in abduction (IRABD) were then simulated.
Results: Maximum impingement-free IR0 was reached with increasing inferior offset in combination with increasing lateralization. Lateralization was the most important variable in increasing impingement-free IRABD. Maximum IRABD was reached at 4-6 mm of lateralization with smaller scapula (−2 to 0 standard deviation). Increasing lateralization up to 12 mm continues to increase IRABD for larger-sized scapula (+1 to +2 standard deviation). Optimal inferior offset and lateralization to maximize IR did have a small loss of external rotation in neutral abduction. There was no loss of external rotation in 60° of abduction.
Conclusion: In a virtual model, the glenosphere position required to maximize IR varied by scapula size. For smaller scapulae, maximum IR0 was reached with a combination of 2.5-mm inferior offset and 0- 4 mm of lateralization. For larger scapulae, maximum IR0 was reached with a combination of 2.5 mm of inferior offset and 4 mm of lateralization. The amount of lateralization required to maximize IRABD also varies by scapula size. Maximum IRABD was reached in smaller scapula with 4-6 mm of lateralization and at least 12 mm of lateralization in larger scapula. These findings may be applied in the clinical decision-making process knowing that impingement-free IR and IRABD can be maximized with combinations of inferior offset and lateralization based on scapula size with minimal effect on external rotation and external rotation in 60° of abduction.

As the number of shoulder arthroplasties performed each year continues to increase, improving patient outcomes continues to be the focus of surgeons.[13] Accurately predicting impingement-free range of motion (ROM), specifically internal rotation (IR), from

Institutional review board approval was not required for this study.

*Corresponding author: Patrick J. Denard, MD, Oregon Shoulder Institute, 2780 E. Barnett Rd Suite 200, Medford, OR 97504, USA.
E-mail address: pjdenard@gmail.com (P.J. Denard).

https://doi.org/10.1016/j.jseint.2024.07.014

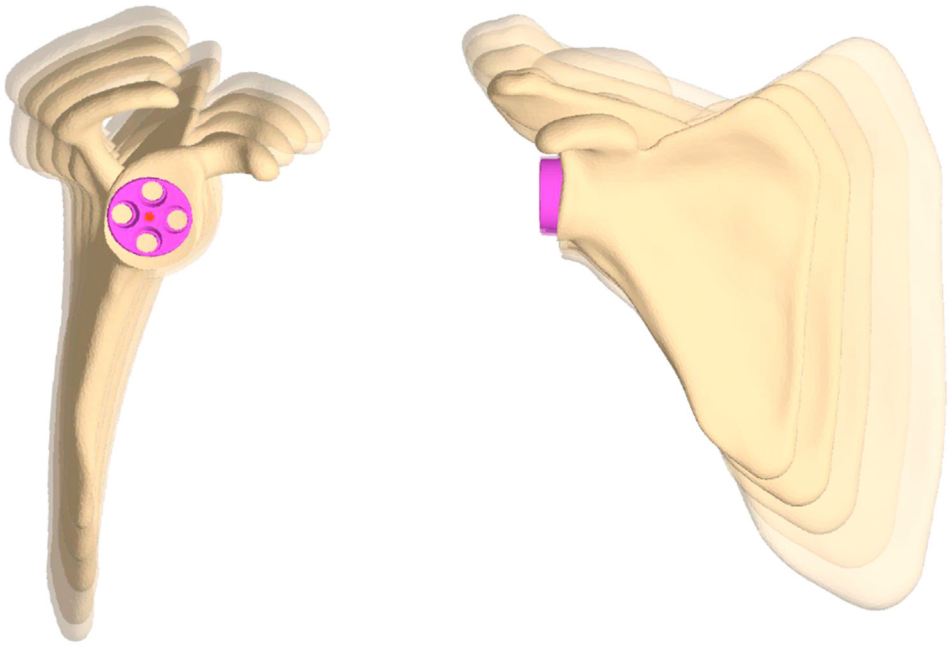

Figure 1 Statistical shape model of 5 scapula sizes including the mean scapula size and 2 standard deviations.

preoperative planning software is one of the final unanswered questions.[26] Loss or minimal improvement of IR after reverse shoulder arthroplasty (RSA) is a known outcome that can have many contributing factors like capsular contracture, subscapularis dysfunction, bony impingement, and various implant factors.[5,8,14-16,21,23] Previous reviews of the literature have aimed to elucidate the most important implant factors for maximizing IR.[8]

Preoperative planning for shoulder arthroplasty allows surgeons to better understand patient anatomy and deformity. Several studies have also shown that surgeons are accurately replicating their preoperative plans intraoperatively.[6,10,24] However, predicting postoperative ROM, specifically IR, from preoperative planning software is one of the final challenges.[2] Several virtual ROM studies have attempted to provide guidelines for glenoid component position and lateralization.[1,11-13,20,28] The majority of these studies have used a model based on only one or very few scapula. Thus, previous studies do not account for variability in scapular size and are limited in the ability to make patient-specific recommendations.

The primary goal of this study was to assess impingement-free IR in a virtual RSA simulation using a Statistical Shape Model (SSM) based on scapula size. The hypothesis was that optimal glenoid-sided implant position and lateralization to achieve maximal impingement-free IR would vary based on scapula size.

Methods

A database including over 10,000 computed tomography (CT) scans, which included the proximal humerus and entire scapula, was queried. CT scans were collected from the Virtual Implant Positioning (VIP; Arthrex, Naples, FL, USA) database to represent the diverse patient population. From this database, a shoulder SSM was created. SSMs are 3-dimensional (3D) geometric models that represent an average shape as well as variations in shape. For the SSM, only right shoulders were considered and left shoulders were mirrored to simulate right shoulders. All patients with previous metal implants were excluded. All CT scans were manually segmented, and 3D surfaces of the humerus and scapula were reconstructed using Mimics (Materialise NV, Leuven, Belgium). To compute the shoulder SSM correspondences between all points, the training set surfaces were determined according to previously described methods for the humerus and scapula correspondences computation.[18] We then applied a Principal Component Analysis to compute the principal modes of variations, eigenvectors with their eigenvalues, of the shoulder SSM. The computed principal modes of variation allow for alterations of the shoulder SSM along the anatomical variations so that a large number of shoulder models were created.

From the database of 10,000 scapulae, 100 were randomly selected and then analyzed to obtain 5 scapulae sizes including the mean and 2 standard deviations. (Fig. 1). Virtual implantation was then conducted and glenohumeral ROM was simulated. For each scapula size model, one glenosphere diameter (33-42 mm) was selected as the best fit based on consensus among 3 fellowship-trained shoulder surgeons. Virtual implantation variables included 1) lateral offset (0-12 mm in 2-mm increments), 2) inferior eccentricity (0, 2.5, 5, and 7.5 mm), and 3) posterior eccentricity (0, 2.5, and 5 mm). (Figs. 2–4) On the humeral side, a 135° inlay component was virtually implanted with a 3-mm polyethylene in all cases.

ROM was simulated in 4 planes using the 3D-reconstructed humerus and scapula: IR in neutral abduction (IR0), IR in 60° of abduction (IRABD), external rotation in neutral abduction (ER0), and external rotation in 60° of abduction (ERABD) (Fig. 5). For each plane, glenohumeral ROM was then simulated to the point of bony impingement (Fig. 6). As the model only simulated bony glenohumeral ROM, the maximum ROM in all planes was capped at 90°. Setting a realistic constraint on maximum ROM in a simulated model was to account for soft tissue constraints.

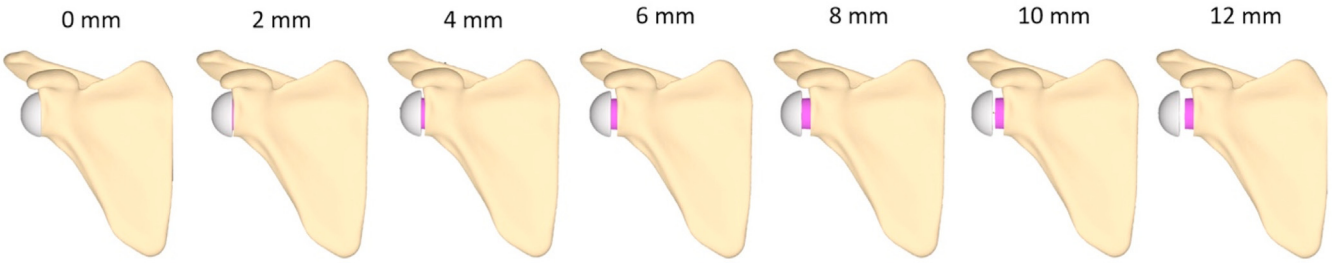

Figure 2 Scapular models demonstrating virtual implantation variables of increasing lateral offset in 2-mm increments.

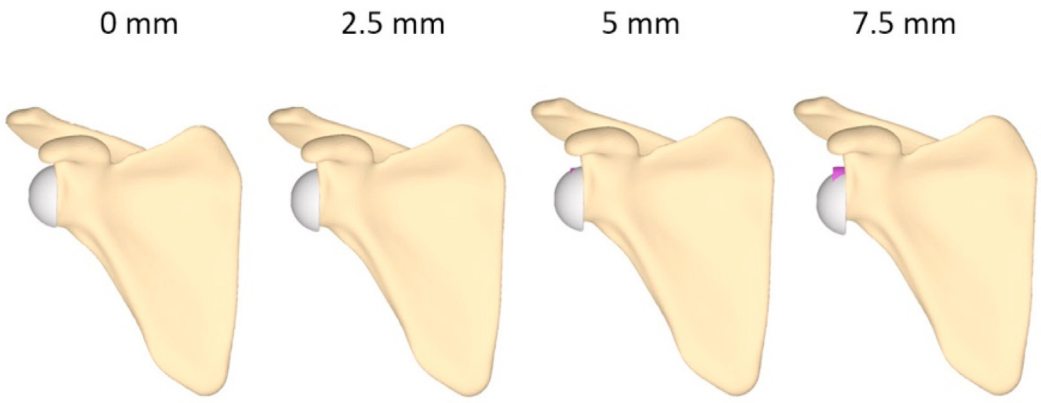

Figure 3 Scapular models demonstrating virtual implantation variables of increasing inferior offset in 2.5-mm increments.

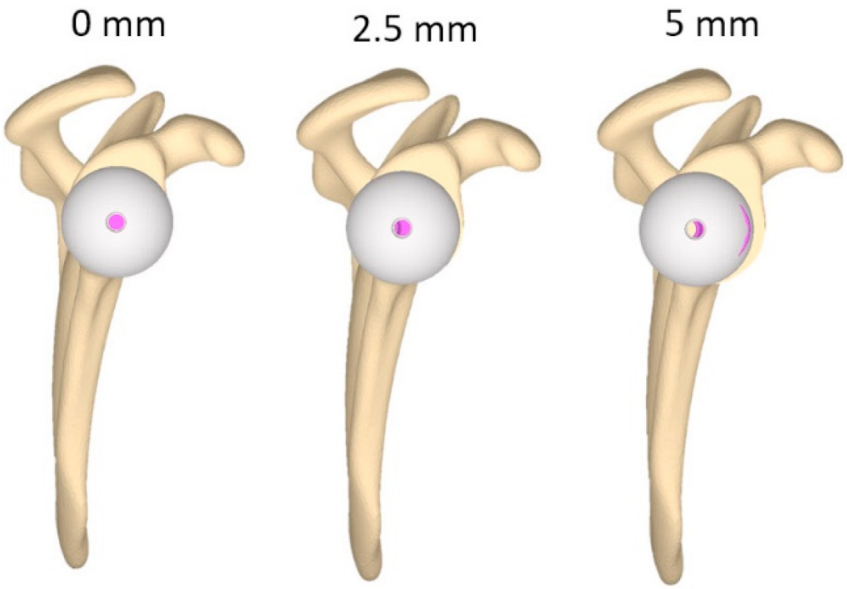

Figure 4 Scapular models demonstrating virtual implantation variables of increasing posterior offset in 2.5-mm increments.

Results

IR0 and ER0

As shown in Fig. 7, increasing inferior offset had a small progressive increase on IR0 until impingement occurred for the −2 standard deviation (SD) to 0 SD size scapula. For the +1 SD and +2 SD size scapula, IR0 reached a maximum with increasing inferior offset up to 7.5 mm. With lateralization alone, IR0 progressively decreased until 8 mm of lateralization, at which point it again increased. Increasing posterior offset without lateralization also decreased IR0. For −2 SD to 0 SD size scapula, maximum IR0 was reached with a combination of 2.5 mm inferior offset and 0 to 4 mm of lateralization. For +1 SD and +2 SD size scapula, maximum IR0 was reached with a combination of 2.5 mm of inferior offset and 4 mm of lateralization (Fig. 8).

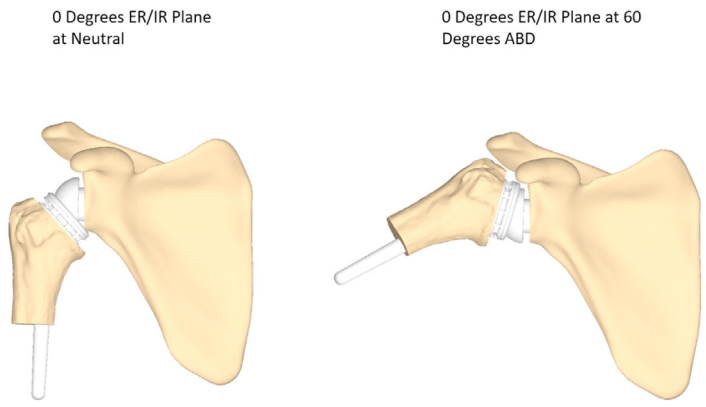

Figure 5 Four planes of simulated range of motion: IR0, ER0, IRABD, and ERABD. *ER0*, external rotation in neutral abduction; *ERABD*, external rotation in 60° of abduction; *IR0*, internal rotation in neutral abduction; *IRABD*, internal rotation in 60° of abduction.

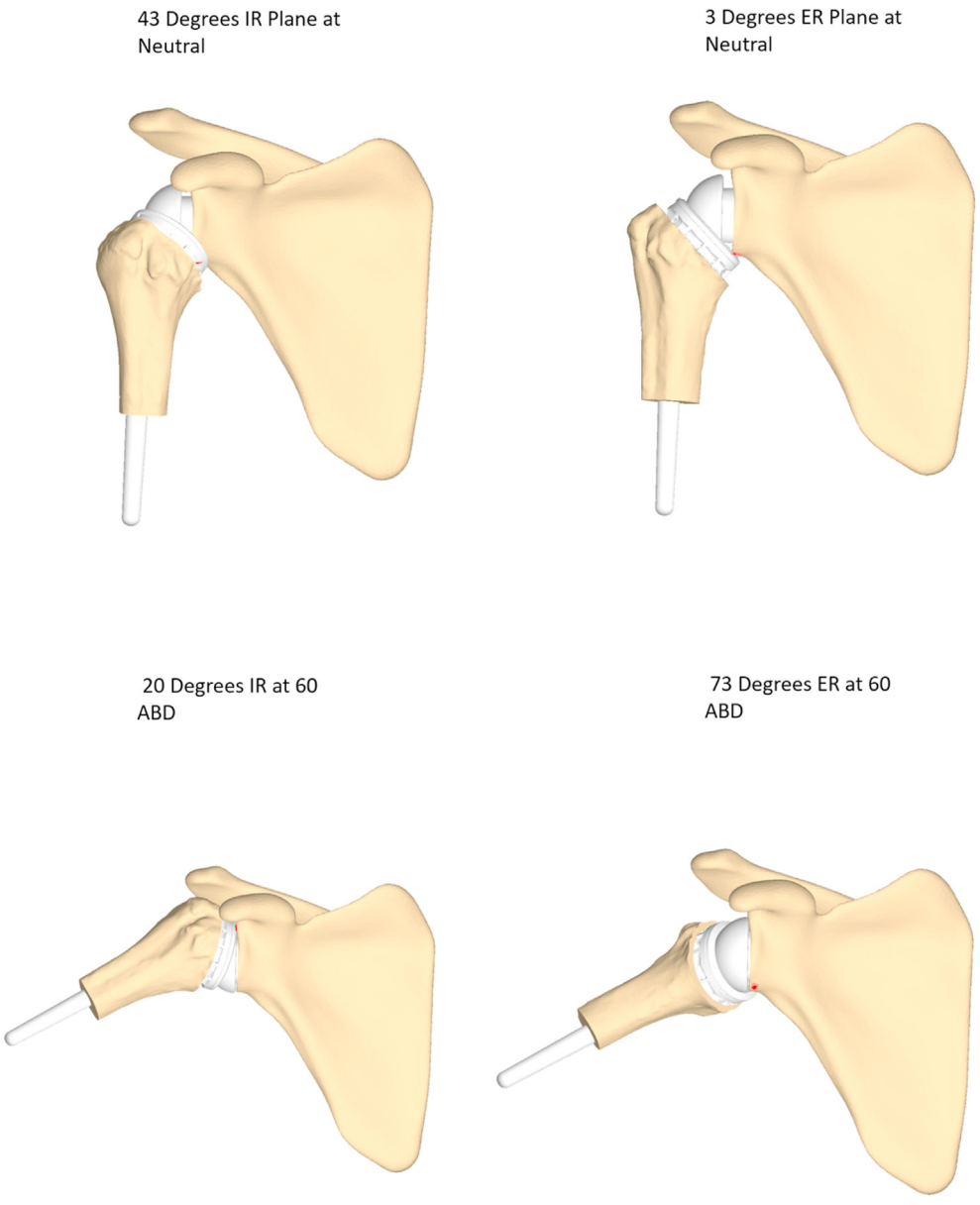

Figure 6 Examples of simulated maximum ROM to the point of bony impingement. *ABD*, abduction; *ER*, external rotation; *IR*, internal rotation; *ROM*, range of motion.

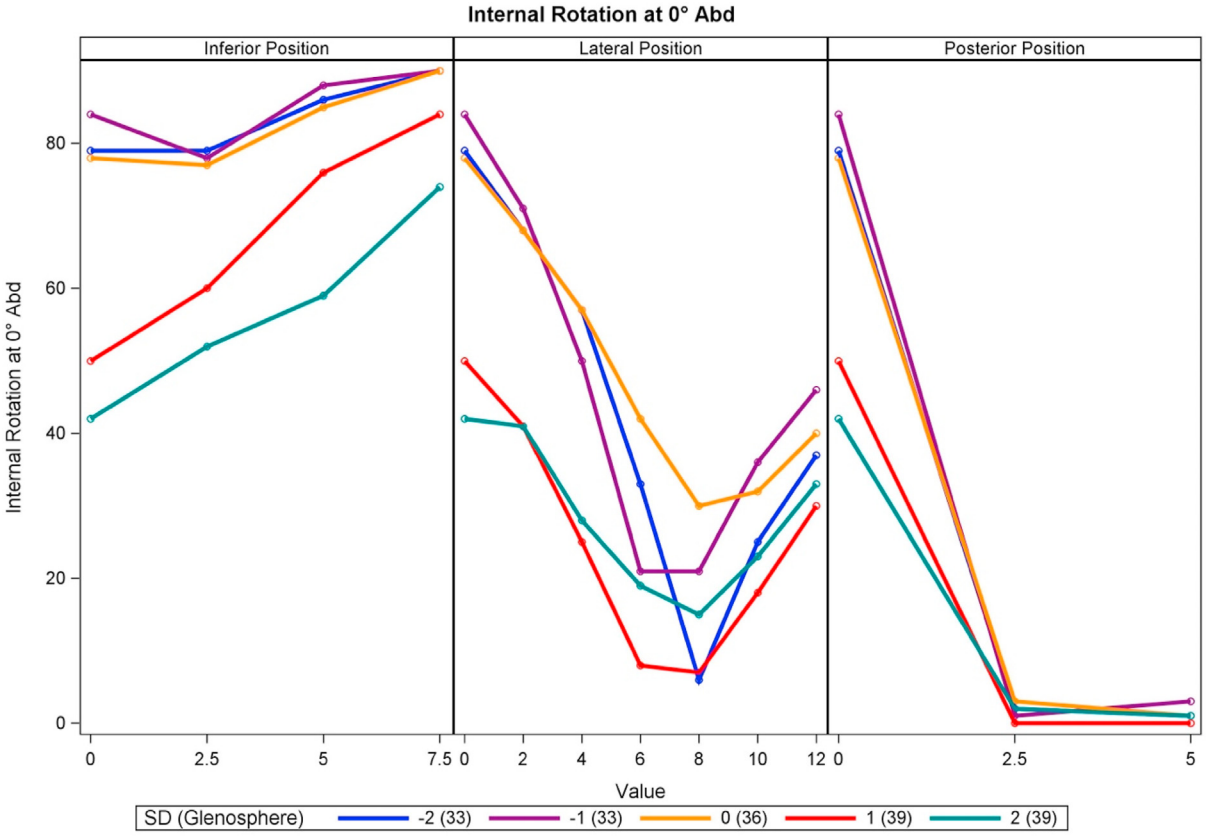

Figure 7 Effect of glenosphere position on IR0. *IR0*, internal rotation in neutral abduction.

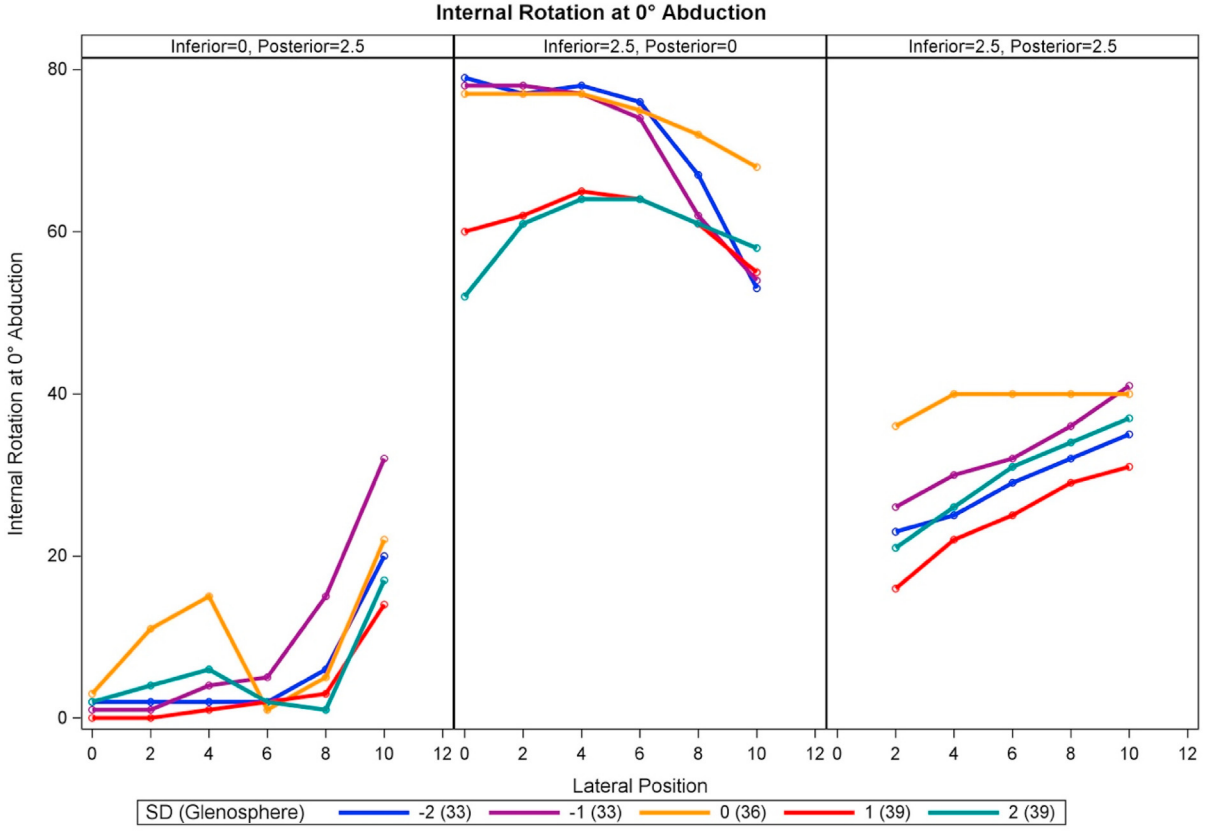

Figure 8 Effect of lateralization in combination with glenosphere position on IR0. *IR0*, internal rotation in neutral abduction.

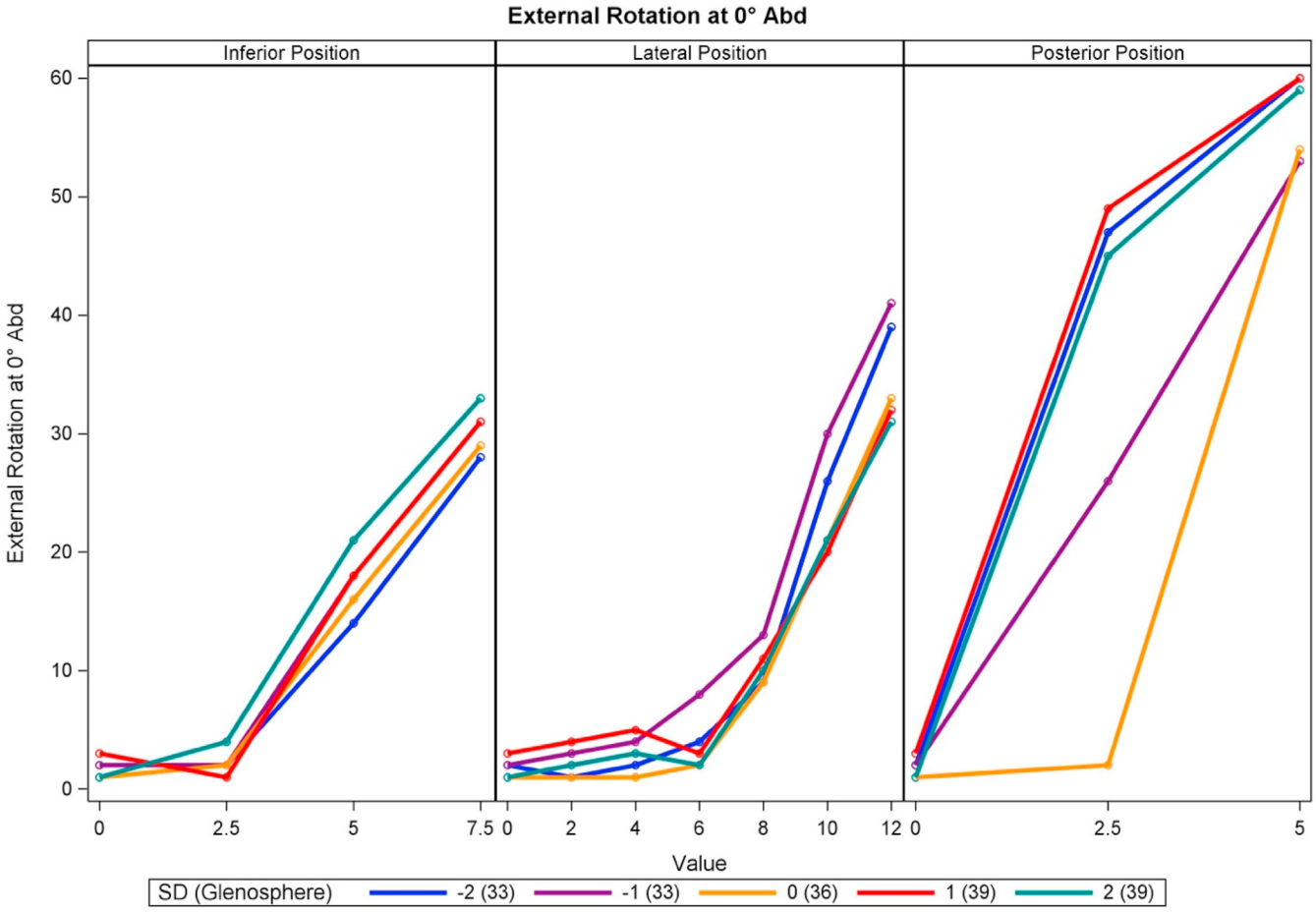

Figure 9 Effect of glenosphere position on ER0. *ER0*, external rotation in neutral abduction.

Increasing inferior offset, lateralization, and posterior offset all led to an increase in ER0 for all scapula sizes. Posterior offset of 5 mm predicted maximal ER0 (Fig. 9). As shown in Fig. 7, posterior offset of 2.5 mm predicted a loss of external rotation (ER) with increasing lateralization. The combination of 2.5 mm of inferior offset and 0 mm of posterior offset predicted an increase of ER0 with increasing lateralization. The combination of 2.5 mm of inferior and 2.5 mm of posterior offset predicted the highest ER0 at 10 mm of lateralization (Fig. 10).

IRABD and ERABD

In the abducted position, lateralization had the largest impact on IRABD. Maximum IRABD was reached at 4 mm of lateralization with the −2 SD and −1 SD size scapula and at 6 mm with the 0 SD size scapula. For scapula sizes +1 SD and +2 SD, lateralization up to 12 mm continued to increase IRABD. Only a slight increase in IRABD was observed with increasing inferior or posterior offset (Fig. 11). Inferior and posterior offset have similar effects leading to increased IRABD with increasing lateralization (Fig. 12). Increasing lateralization increased ERABD with 0 mm of inferior and posterior offset. Increased posterior and inferior offset beyond 0 mm had minimal effect on ERABD (Fig. 13).

Discussion

The most important finding of this virtual ROM study was that variations in glenoid-sided implant position required to maximize IR does vary by scapula size. In a neutral arm position, maximum IR0 was reached with a combination of 2.5-mm inferior offset and 0- 4 mm of lateralization for −2 SD to 0 SD scapula. For +1 SD and +2 SD scapula, maximum IR0 was reached with a combination of 2.5 mm of inferior offset and 4 mm of lateralization. Again, this demonstrates that smaller and larger scapula necessitate different glenosphere positions when maximizing IR0 is the goal. In the abducted position, our virtual model demonstrated that increased lateralization is most important in maximizing IRABD compared to inferior or posterior offset. It was also shown that the amount of lateralization required to maximize IRABD varies by scapula size. For the 2 smallest scapula, maximal IR0 was achieved with 4 mm of lateralization, for the mean size 6 mm was required, whereas for larger scapula IR0 continued to increase out to 12 mm and did not reach a ceiling. Furthermore, our virtual model demonstrated no loss in ERABD with changes to implant position to maximize IRABD. These findings may have implications for patient-specific planning considerations.

Loss or minimal improvement in IR after RSA is a known outcome that can have many contributing factors like capsular contracture, subscapularis dysfunction, bony impingement, and many implant factors.[8,16,21,23] Previous reviews of the literature have aimed to elucidate the most important implant factors for maximizing IR. Improved IR is associated with: lower humeral neck shaft angle, increased glenoid lateralization, decreased humeral retroversion, inferior baseplate position, inferior baseplate tilt, and subscapularis repair.[8] A multicenter retrospective review by Werner et al[27] studied active IR after RSA in a 135° humeral inlay

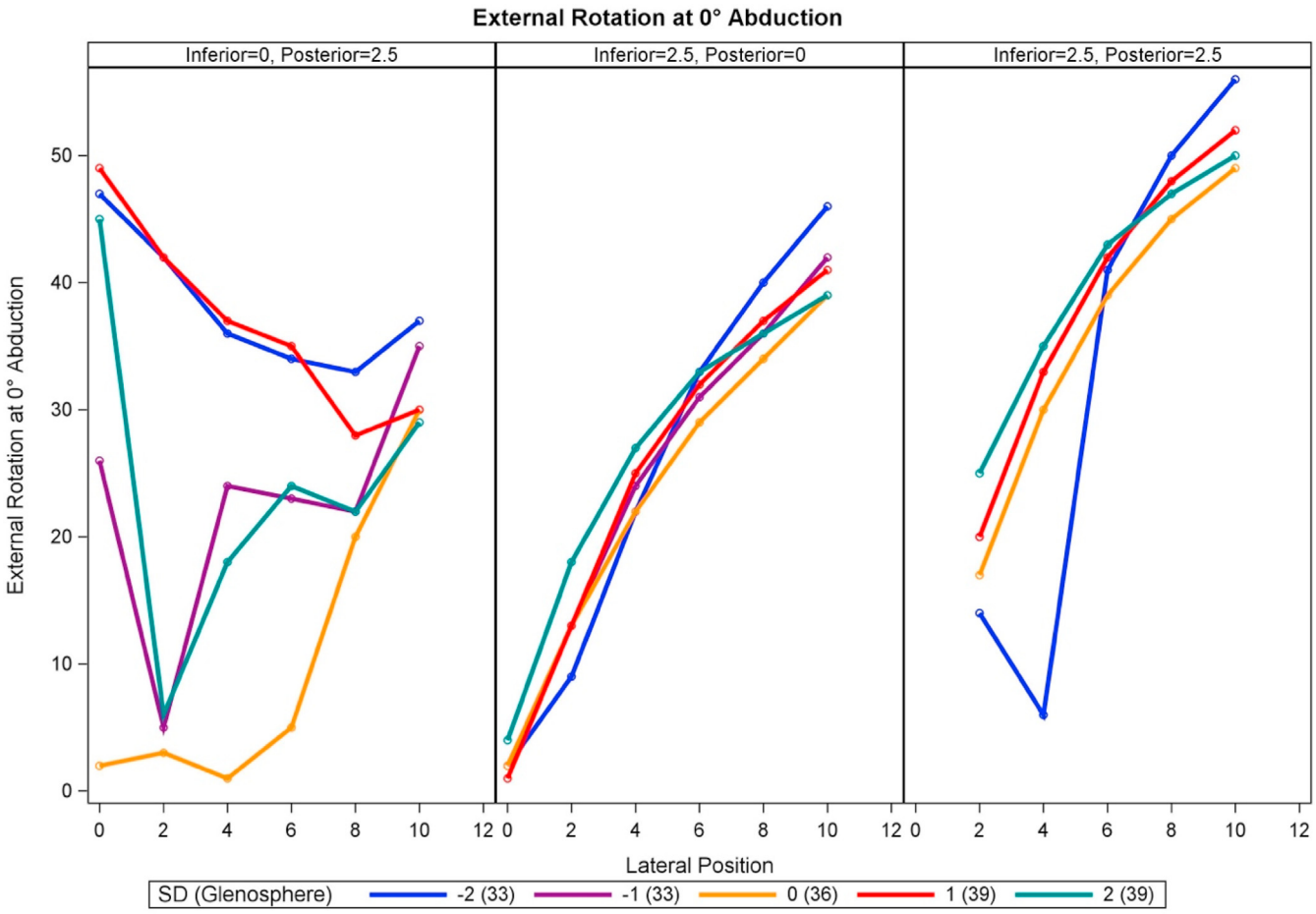

Figure 10 Effect of lateralization in combination with glenosphere position on ER0. *ER0*, external rotation in neutral abduction.

prosthesis with varying amounts of glenoid lateralization. They found that increasing glenoid-sided lateralization improved IR, with 6- 8 mm yielding the best results; however, even with a lateralized glenoid approximately 50% of patients fail to achieve functional IR after RSA. Variations in scapula size based on patient sex or height were not analyzed in the study. Almost half of those patients failed to achieve functional IR, this could be related to the amount of lateralization not tailored to variations in patient scapula size and morphology. Our findings confirm that increased lateralization with glenosphere size matched to scapula size and inferior offset maximizes IR0 in a virtual model.

Similar to our findings, Werner et al showed with their virtual model that increased lateralization had the most effect on increased total ROM.[28] However, they only examined lateralization out to 5 mm in 1 scapula model. Keener et al also showed a significant increase in ROM in all measured planes with increased lateralization out to a maximum of 10 mm in 10 consecutive specimens.[12] Virani et al's virtual model of a single scapula found that increasing lateralization and inferior offset maximizes IR, similar to our findings.[25] Maximum IRABD has been analyzed in a previous virtual model conducted by Li et al which demonstrated increased IR with increased lateralization. Li et al also showed that increasing inferior offset increased IRABD.[16] Many activities of daily living require the arm to be slightly abducted; therefore, these models support clinically meaningful predictions in ROM.

Anthropometric studies have been conducted which prove that height can be accurately predicted from scapula size; therefore, patient height can be used as a guide when selecting glenosphere size.[4,7] Appropriately matched glenosphere size to patient anatomy can maximize ROM by reducing bony impingement.[19] Matuski et al found no significant differences in postoperative ROM between 38–, 42–, and 46–mm-diameter glenospheres selected based on surgeon preference in a 145° neck shaft angle prosthesis. They found that small- and tall-stature patients had significantly less postoperative ER gain compared to average-stature patients.[17] For small-stature patients, the 38-mm diameter glenosphere may increase risk for bony impingement, resulting in a loss of ER compared to average-stature patients. Height-matched glenosphere size correlates with improved patient outcome scores.[22] In our virtual model, we found that smaller scapulae (−2 to 0 SD) would achieve maximum IR with 0 to 4 mm of lateralization with 2.5 mm inferior offset. Larger scapulae (+1 to +2 SD) reached maximum IR with lateralization of 4 mm with 2.5 mm inferior offset. Our virtual model findings can be applied in the clinical decision-making process knowing that IR is maximized with at least 4 mm of lateralization plus 2.5 mm inferior offset in small- and average-sized scapula. Future work may therefore include guidelines of lateralization and inferior position based on predictive modeling of the scapula.

While scapula size and therefore glenoid size varies based on patient height, other variations in scapula and humeral anatomy can affect optimal implant size and position for maximizing ROM.[3,9] Variations in the anatomy of the coracoid, acromion, scapular neck length, glenoid inclination, and greater/lesser tuberosities can all affect maximum ROM before bony impingement. All of these variations may be considerations when selecting the appropriate

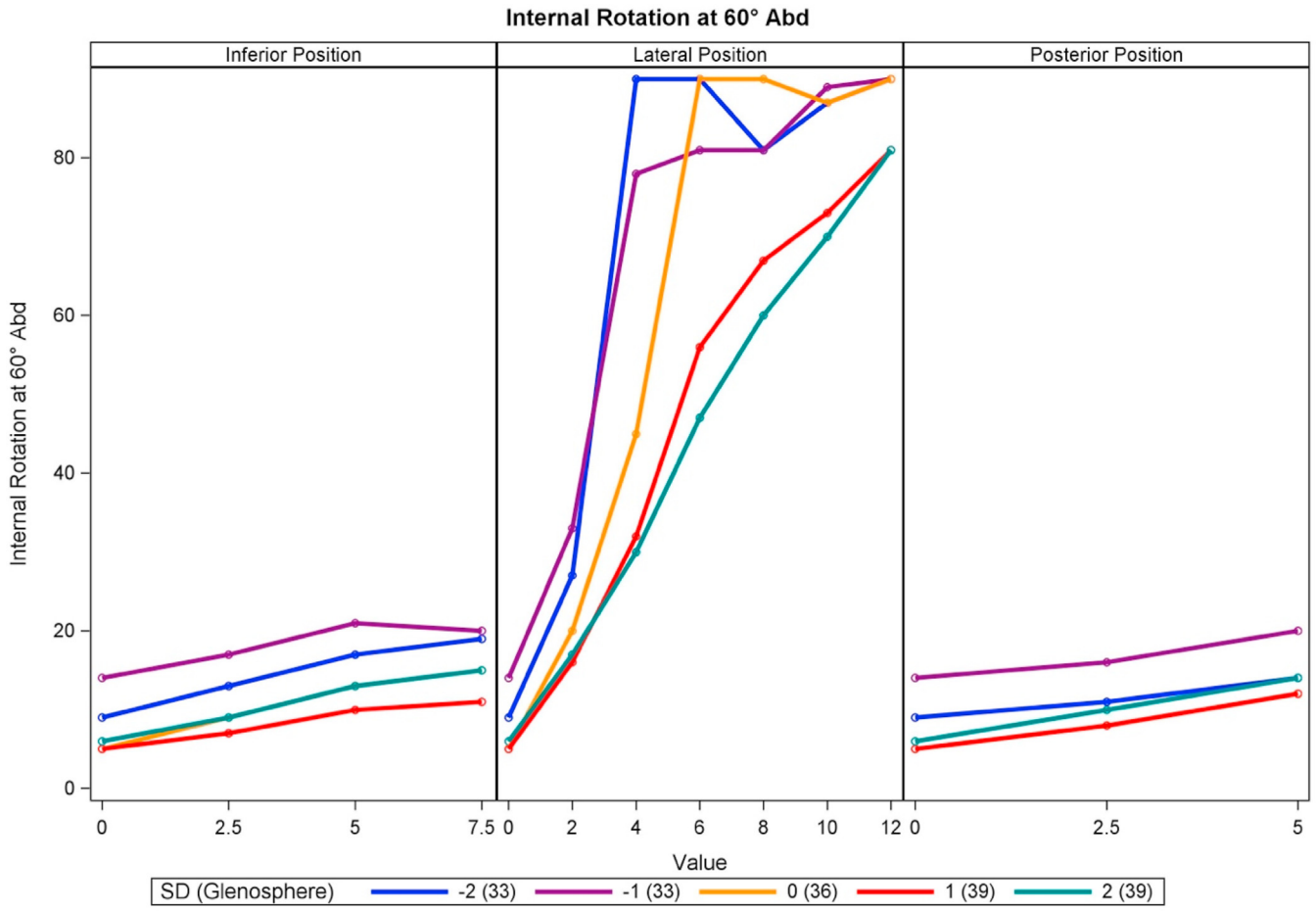

Figure 11 Effect of glenosphere position on IRABD. *IRABD*, internal rotation in 60° of abduction.

implant size and position, as well as the functional goals of each patient. Further research is therefore needed in this area as our model only accounted for scapula size.

There are several limitations of this study. The virtual model is based on a single 135° neck shaft angle inlay design prosthesis implant. Our findings may not be translatable to other implant systems. Likewise, our model does not account for variation in humeral version. It has been shown that humeral version impacts IR.[8] Our virtual model does not account for soft tissue constraint or soft tissue impingement. This could overestimate maximum ROM before clinically significant impingement in vivo. We attempted to control for this by setting realistic maximum ROM. Another limitation is that this virtual model had no variation in humeral side anatomy. Bony impingement with the greater tuberosity and acromion with abduction as well as between the greater tuberosity and coracoid with forward flexion, abduction and IR may occur. We controlled for patient variability on the scapular side, but not the humeral side. Finally, our virtual model does not account for motion through the scapulothoracic joint. The orientation of the scapula was not taken into account for in our model which can have an effect when bony impingement is occurring.

Conclusion

In a virtual model, the glenosphere position required to maximize IR varied by scapula size. For smaller scapulae, maximum IR0 was reached with a combination of 2.5 mm of inferior offset and 0-4 mm of lateralization. For larger scapulae, maximum IR0 was reached with a combination of 2.5 mm of inferior offset and 4 mm of lateralization. The amount of lateralization required to maximize IRABD also varies by scapula size. Maximum IRABD was reached in smaller scapula with 4 to 6 mm of lateralization and at least 12 mm of lateralization in larger scapula. These findings may be applied in the clinical decision-making process knowing that impingement-free IR and IRABD can be maximized with combinations of inferior offset and lateralization based on scapula size with minimal effect on ER and ERABD.

Acknowledgments

The authors would like to acknowledge David Knopf, Siddhant Thakur, Angel Esquilin Lozada, Chris Cronin, Scott Doody, and Steven De Leon in affiliation with Arthrex Inc., Naples, FL, USA.

Disclaimers:

Funding: No funding was disclosed by the authors.
Conflicts of interest: Dr. Alexandre Lädermann reports being a paid consultant for Arthrex, Stryker, Medacta, Enovis; receives royalties from Stryker and Medacta; is the cofounder of FORE, Med4Cast, and BeeMed; has stock options in Medacta and Follow Health; and is a board member at the French Arthroscopic Society. Dr. Brian C Werner is a paid speaker and paid consultant at Arthrex and reports receiving research funding from the same; received research

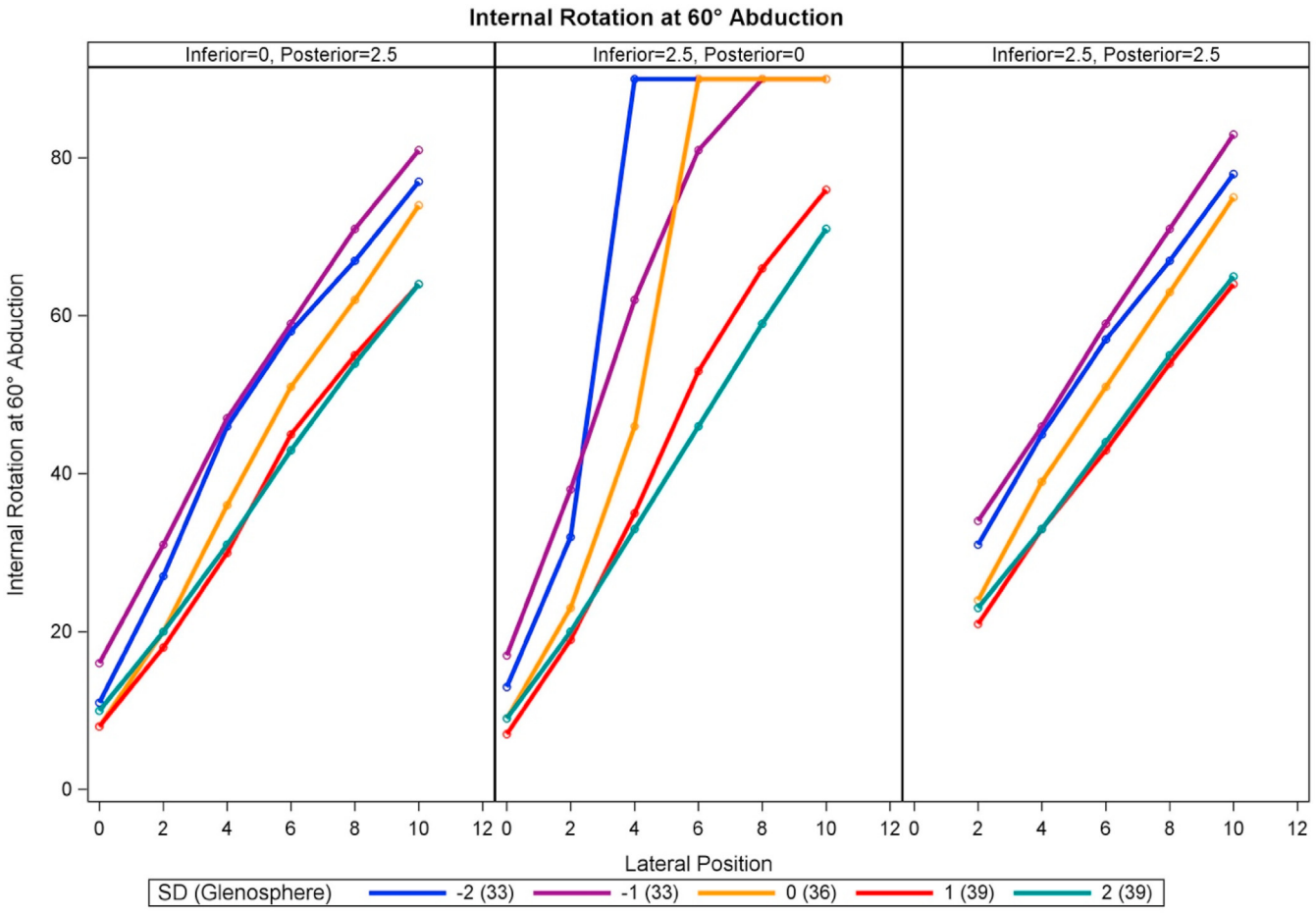

Figure 12 Effect of lateralization in combination with glenosphere position on IRABD. *IRABD*, internal rotation in 60° of abduction.

funding from Zimmer Biomet, Exactech, and Pacira; and is a paid consultant for Lifenet Health. Dr. Stefan Greiner reports being a paid speaker and paid consultant at Arthrex. Dr. Patrick J Denard, MD reports being a paid speaker and paid consultant at Arthrex and receiving royalties from the same and owns stock at PT Genie and Kaliber Labs. Dr. Albert Lin reports board or committee membership at AAOS, International Society of Arthroscopy, Knee Surgery, and Orthopaedic Sports Medicine, American Orthopaedic Association, American Orthopaedic Society for Sports Medicine, and American Shoulder and Elbow Surgeons; editorial or governing board membership at Arthroscopy, Knee Surgery, Sports Traumatology, Arthroscopy, and Annals in Joint; and being a paid consultant at Arthrex and Tornier. Dr. Anthony Romeo reports receiving royalties from Arthrex and being a paid presenter and paid consultant at the same; editorial or governing board membership at Orthopedics Today, Orthopedics, SAGE, SLACK Incorporated; stock or stock options at Paragen Technologies; receiving research support and royalties from Vertex; and Financial or Material Support from Publishers: Aunders/Mosby-Elsevier. Dr. Anup Shah reports being an education/research consultant at Arthrex and receiving royalties from Medacta. Dr. Asheesh Bedi reports being a consultant and receiving royalties from Arthrex. Dr. Benjamin W. Sears reports being a consultant and receiving royalties from the United Orthopaedic Corporation, Shoulder Innovations, BioPoly, and Aeuvumed and receiving research/funding support from Arthrex, Exactech, Stryker, and FX Solutions. Dr. Bradford Parsons reports being a consultant and receiving royalties from Arthrex and being an editor at JBJS reviews. Dr. Brandon Erickson reports board or committee membership at AAOS, American Orthopaedic Society for Sports Medicine, American Shoulder and Elbow Surgeons; receiving research support and being a paid consultant at Arthrex; receiving research support from Johnson & Johnson Company, DePuy, Smith & Nephew, Stryker, and Linvatec; and editorial or governing board membership at PLOS One. Dr. Bruce Miller reports editorial or governing board membership at AJSM; is a paid consultant at Arthrex; and receives royalties from FH Orthopedics. Dr. Christopher O'Grady reports being an education consultant/speaker at Arthrex, Stryker, Smith and Nephew, and Mitek. Dr. Daniel Davis reports being a paid consultant and a paid presenter/speaker at Arthrex; owning stock or stock options at Catalyst OrthoScience; and board membership at the Pennsylvania Orthopaedic Society and the Philadelphia Orthopaedic Society. Dr. David Lutton reports being a paid consultant, paid speaker or presenter at Arthrex; paid speaker or presenter at Avanos; and a reviwer (not editor) at CORE. Dr. Dirk Petre reports being a paid consultant, paid presenter/speaker at Arthrex and receives research support from the same. Dr. Justin Griffin reports receiving research support, royalties from Arthrex and is a paid speaker at the same and receives publishing royalties from Springer. Dr. John Tokish reports being a paid consultant and paid presenter or speaker for and receiving IP royalties from Arthrex; board or committee membership at Arthroscopy Association of North America; receives financial or material support from and is an editorial or governing board member at Journal of Shoulder and Elbow Surgery; and is an editorial or governing board member at Orthopedics Today. Dr. Jorn Steinbeck is a reviewer at the Journal of Shoulder and Elbow

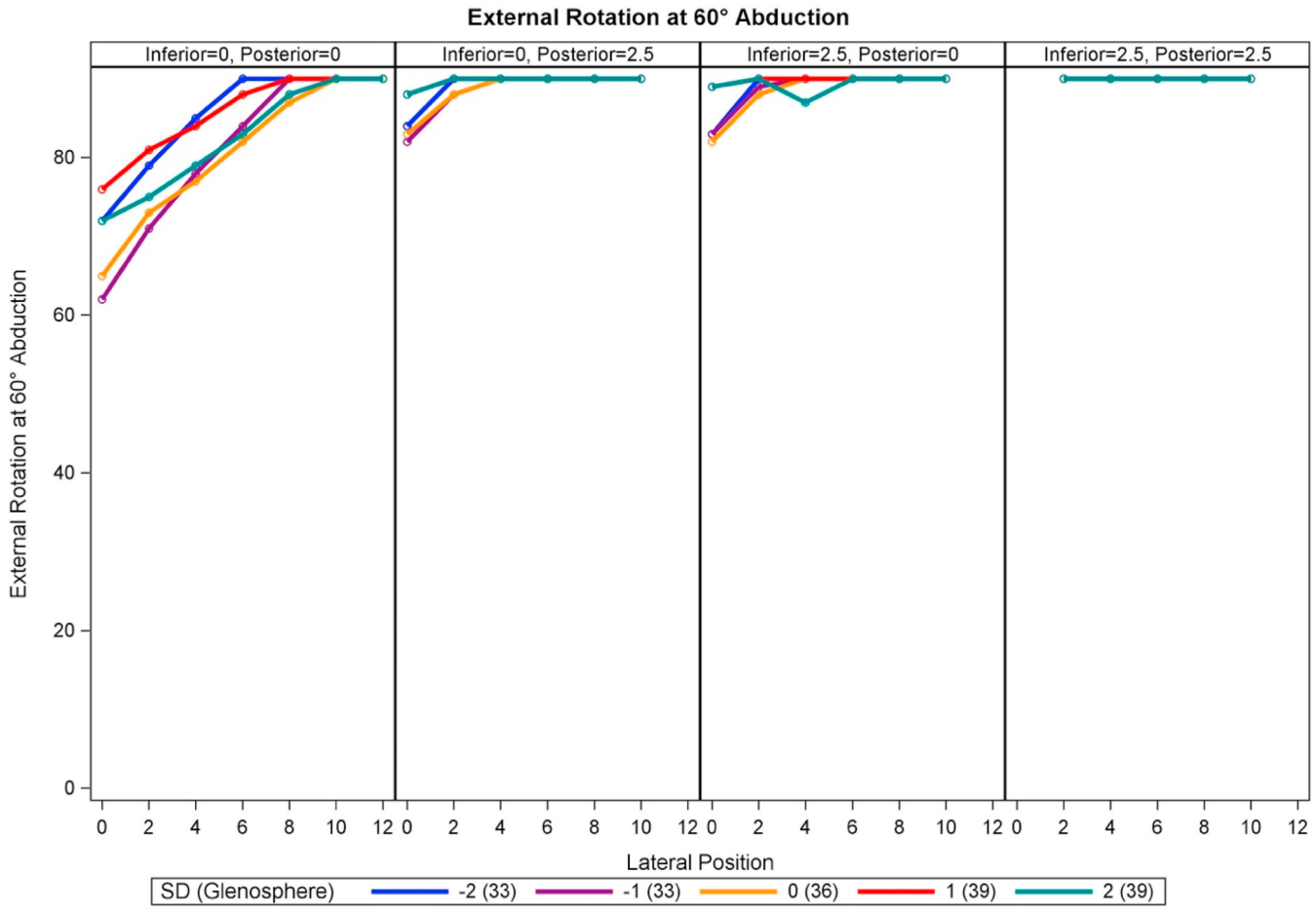

Figure 13 Effect of lateralization in combination with glenosphere position on ERABD. *ERABD*, external rotation in 60° of abduction.

Surgery and Journal of Bone and Joint Surgery and is a consultant at Arthrex. Dr. Julia Lee reports the following Arthrex, Inc.: Consulting and medical education; American Shoulder Elbow Surgeons: committee member Dr. Kevin Farmer reports board or committee membership at the American Orthopaedic Society for Sports Medicine Florida Orthopaedic Society; being a paid consultant, paid presenter or speaker at Arthrex; being a paid consultant at Exactech. Dr. Mathew Provencher reports receiving royalties from Arthrex, Arthrosurface, Responsive Arthroscopy (2020), and Anika Therapeutics; receiving consulting fees from Arthrex, Joint Restoration Foundation, Zimmer Biomet Holdings, and Arthrosurface; grants from the Department of Defense, the National Institute of Health, and DJO (2020); receiving honoraria from Flexion Therapeutics; being editorial board or governing board member at SLACK; board or committee membership at American Association of Nurse Anesthesiology, American Academy of Orthopaedic Surgeons, American Orthopaedic Society for Sports Medicine, American Shoulder and Elbow Surgeons, San Diego Shoulder Institute, and Society of Military Orthopaedic Surgeons; and medical board of trustees (through 2018) membership at the Musculoskeletal Transplant Foundation. Dr. Michael Bercik reports board or committee membership at American Shoulder and Elbow Surgeons and being a paid consultant for Arthrex and WRS Specialists. Dr. Michael Kissenberth reports being a paid consultant at Arthrex; receiving financial or material support from the Hawkins Foundation and being a board member for the same. Dr. Patric Raiss reports being a paid consultant for Arthrex and a shareholder at Zurimed Technologies AG. Dr. Peter Habermeyer reports receiving royalties from Arthrex. Dr. Philipp Moroder reports receiving royalties from Arthrex, Medacta, and Alyve Medical and being a consultant for the same. Dr. Robert Creighton reports board or committee membership at the American Board of Orthopaedic Surgery, American Orthopaedic Society for Sports Medicine, and American Shoulder and Elbow Surgeons; being a paid presenter or speaker at Arthrex, receiving research support, and other financial or material support from the same; receiving other financial or material support from Breg, Johnson & Johnson, and Smith & Nephew; and editorial or governing board membership at Orthopedics Today and SLACK Incorporated. Dr. G. Russell Huffman reports speakers bureau/paid presentations, paid consultant at Arthrex and LIMA; stock or stock options at Catalyst; and receiving research support from PI: LIMA IDE. Dr. Samuel Harmsen reports receiving royalties and research support from Arthrex and being paid consultant, paid presenter or speaker for the same; receiving royalties and being a paid consultant for Embody; paid consultant and paid presenter for Enovis; royalties, stock or stock options at Genesis Software Innovations; royalties, paid consultant, paid presenter or speaker at Shoulder Innovations, Inc; paid consultant, paid presenter or speaker, stock or stock options at Zimmer US Inc. Dr. Sven Lichtenberg reports editorial or governing board membership at Archives of Orthopaedic and Trauma Surgery, Journals of Shoulder and Elbow Surgery, and Knee Surgery, Sports Traumatology, Arthroscopy and paid consultant, paid presenter or speaker at Arthrex and Exactech; and IP royalties at Arthrex. Dr. Tim Lenters reports being a paid

consultant at Arthrex; receiving research support from Irispet; and social media committee membership at the American Academy of Orthopaedic Surgeons. Dr. Matthew Tyrrell Burrus reports being a paid consultant, paid presenter or speaker at Arthrex and receives research support from the same and is an editorial or governing board member at Arthroscopy. Dr. Tyler Brolin reports board or committee membership at American Academy of Orthopaedic Surgeons and American Shoulder and Elbow Surgeons; receives IP royalties, paid consultant, research support from Arthrex and Zimmer; receives publishing royalties, financial or material support from Elsevier; receives research support from Orthofix; and has editorial or governing board membership at Orthopedic Clinics of North America. The other authors, their immediate families, and any research foundations with which they are affiliated have not received any financial payments or other benefits from any commercial entity related to the subject of this article.

References

1. Arenas-Miquelez A, Murphy RJ, Rosa A, Caironi D, Zumstein MA. Impact of humeral and glenoid component variations on range of motion in reverse geometry total shoulder arthroplasty: a standardized computer model study. J Shoulder Elbow Surg 2021;30:763-71. https://doi.org/10.1016/j.jse.2020.07.026.
2. Berhouet J, Samargandi R, Favard L, Turbillon C, Jacquot A, Gauci M-O. The real post-operative range of motion differs from the virtual pre-operative planned range of motion in reverse shoulder arthroplasty. J Pers Med 2023;13:765. https://doi.org/10.3390/jpm13050765.
3. Callegari J, Haidamous G, Lädermann A, Phillips C, Tracy S, Denard P. Factors influencing appropriate implant selection and position in reverse total shoulder arthroplasty. Orthop Clin North Am 2021;52:157-66. https://doi.org/10.1016/j.ocl.2020.12.006.
4. Campobasso CP, Di Vella G, Introna F. Using scapular measurements in regression formulae for the estimation of stature. Boll Della Soc Ital Biol Sper 1998;74:75-82.
5. Collin P, Rol M, Muniandy M, Gain S, Lädermann A, Ode G. Relationship between postoperative integrity of subscapularis tendon and functional outcome in reverse shoulder arthroplasty. J Shoulder Elbow Surg 2022;31:63-71. https://doi.org/10.1016/j.jse.2021.05.024.
6. Dallalana R, McMahon R, East B, Geraghty L. Accuracy of patient-specific instrumentation in anatomic and reverse total shoulder arthroplasty. Int J Shoulder Surg 2016;10:59. https://doi.org/10.4103/0973-6042.180717.
7. Giurazza F, Del Vescovo R, Schena E, Cazzato RL, D'Agostino F, Grasso RF, et al. Stature estimation from scapular measurements by CT scan evaluation in an Italian population. Leg Med 2013;15:202-8. https://doi.org/10.1016/j.legalmed.2013.01.002.
8. Gruber MD, Kirloskar KM, Werner BC, Lädermann A, Denard PJ. Factors associated with internal rotation after reverse shoulder arthroplasty: a Narrative review. JSES Rev Rep Tech 2022;2:117-24. https://doi.org/10.1016/j.xrrt.2021.12.007.
9. Haidamous G, Lädermann A, Hartzler RU, Parsons BO, Lederman ES, Tokish JM, et al. Radiographic parameters associated with excellent versus poor range of motion outcomes following reverse shoulder arthroplasty. Shoulder Elbow 2022;14:39-47. https://doi.org/10.1177/1758573220936234.
10. Heylen S, Van Haver A, Vuylsteke K, Declercq G, Verborgt O. Patient-specific instrument guidance of glenoid component implantation reduces inclination variability in total and reverse shoulder arthroplasty. J Shoulder Elbow Surg 2016;25:186-92. https://doi.org/10.1016/j.jse.2015.07.024.
11. Huish EG, Athwal GS, Neyton L, Walch G. Adjusting implant size and position can improve internal rotation after reverse total shoulder arthroplasty in a three-dimensional computational model. Clin Orthop 2021;479:198-204. https://doi.org/10.1097/CORR.0000000000001526.
12. Keener JD, Patterson BM, Orvets N, Aleem AW, Chamberlain AM. Optimizing reverse shoulder arthroplasty component position in the setting of advanced arthritis with posterior glenoid erosion: a computer-enhanced range of motion analysis. J Shoulder Elbow Surg 2018;27:339-49. https://doi.org/10.1016/j.jse.2017.09.011.
13. Kim S-J, Jang S, Jung K-H, Kim YS, Lee S-J, Yoo Y. Analysis of impingement-free range of motion of the glenohumeral joint after reverse total shoulder arthroplasty using three different implant models. J Orthop Sci 2019;24:87-94. https://doi.org/10.1016/j.jos.2018.08.016.
14. Lädermann A, Denard PJ, Boileau P, Farron A, Deransart P, Walch G. What is the best glenoid configuration in onlay reverse shoulder arthroplasty? Int Orthop 2018;42:1339-46. https://doi.org/10.1007/s00264-018-3850-x.
15. Lädermann A, Denard PJ, Collin P, Zbinden O, Chiu JC-H, Boileau P, et al. Effect of humeral stem and glenosphere designs on range of motion and muscle length in reverse shoulder arthroplasty. Int Orthop 2020;44:519-30. https://doi.org/10.1007/s00264-019-04463-2.
16. Li X, Knutson Z, Choi D, Lobatto D, Lipman J, Craig EV, et al. Effects of glenosphere positioning on impingement-free internal and external rotation after reverse total shoulder arthroplasty. J Shoulder Elbow Surg 2013;22:807-13. https://doi.org/10.1016/j.jse.2012.07.013.
17. Matsuki K, King JJ, Wright TW, Schoch BS. Outcomes of reverse shoulder arthroplasty in small- and large-stature patients. J Shoulder Elbow Surg 2018;27:808-15. https://doi.org/10.1016/j.jse.2017.11.011.
18. Mayya M, Poltaretskyi S, Hamitouche C, Chaoui J. Mesh correspondence improvement using regional affine registration: application to statistical shape model of the scapula. IRBM 2015;36:220-32. https://doi.org/10.1016/j.irbm.2015.06.003.
19. Müller AM, Born M, Jung C, Flury M, Kolling C, Schwyzer H-K, et al. Glenosphere size in reverse shoulder arthroplasty: is larger better for external rotation and abduction strength? J Shoulder Elbow Surg 2018;27:44-52. https://doi.org/10.1016/j.jse.2017.06.002.
20. Nakazawa K, Manaka T, Minoda Y, Hirakawa Y, Ito Y, Iio R, et al. Impact of constrained humeral liner on impingement-free range of motion and impingement type in reverse shoulder arthroplasty using a computer simulation. J Shoulder Elbow Surg 2023;33:181-91. https://doi.org/10.1016/j.jse.2023.06.038.
21. Rol M, Favard L, Berhouet J. Factors associated with internal rotation outcomes after reverse shoulder arthroplasty. Orthop Traumatol Surg Res 2019;105:1515-9. https://doi.org/10.1016/j.otsr.2019.07.024.
22. Schoch BS, Vasilopoulos T, LaChaud G, Wright TW, Roche C, King JJ, et al. Optimal glenosphere size cannot be determined by patient height. J Shoulder Elbow Surg 2020;29:258-65. https://doi.org/10.1016/j.jse.2019.07.003.
23. Triplet JJ, Kurowicki J, Berglund DD, Rosas S, Horn BJ, Levy JC. Loss of functional internal rotation following various combinations of Bilateral shoulder arthroplasty. Surg Technol Int 2018;33:326-31.
24. Verborgt O, Hachem AI, Eid K, Vuylsteke K, Ferrand M, Hardy P. Accuracy of patient-specific guided implantation of the glenoid component in reversed shoulder arthroplasty. Orthop Traumatol Surg Res 2018;104:767-72. https://doi.org/10.1016/j.otsr.2018.01.010.
25. Virani NA, Cabezas A, Gutiérrez S, Santoni BG, Otto R, Frankle M. Reverse shoulder arthroplasty components and surgical techniques that restore glenohumeral motion. J Shoulder Elbow Surg 2013;22:179-87. https://doi.org/10.1016/j.jse.2012.02.004.
26. Wagner ER, Farley KX, Higgins I, Wilson JM, Daly CA, Gottschalk MB. The incidence of shoulder arthroplasty: rise and future projections compared with hip and knee arthroplasty. J Shoulder Elbow Surg 2020;29:2601-9. https://doi.org/10.1016/j.jse.2020.03.049.
27. Werner BC, Lederman E, Gobezie R, Denard PJ. Glenoid lateralization influences active internal rotation after reverse shoulder arthroplasty. J Shoulder Elbow Surg 2021;30:2498-505. https://doi.org/10.1016/j.jse.2021.02.021.
28. Werner BS, Chaoui J, Walch G. The influence of humeral neck shaft angle and glenoid lateralization on range of motion in reverse shoulder arthroplasty. J Shoulder Elbow Surg 2017;26:1726-31. https://doi.org/10.1016/j.jse.2017.03.032.